Please select category below:
Normal Paper ☒
Student Paper ☐
Young Engineer Paper ☐

Satellite Attitude Control with a six-Control Moment Gyro Cluster tested under Microgravity Conditions

Hélène Evain [1], Daniel Alazard [2], Mathieu Rognant [3], Thomas Solatges [4], Antoine Brunet [3], Jean Mignot [1], Nicolas Rodriguez [2] and Adrien Dias Ribeiro [3]

[1] *CNES, Toulouse, France*
[2] *ISAE SUPAERO, Toulouse, France*
[3] *ONERA, Toulouse, France*
[4] *SITIA, Nantes, France*

Abstract

The attitude control of a satellite equipped with a six-Control Moment Gyro (CMG) cluster is studied, taking into account CMG failure cases and constraints like actuator saturation and real-time aspects. The design of the steering law that allocates the required torques among the actuators is made complex by singularities (gimbal angles of the CMGs where no torque can be created along an axis). This paper describes the problem of a constrained allocation applied to the CMG system, and explains the selected solution. An experimental setup with six CMGs has been designed. It calculates in real-time the attitude guidance laws and control loop. Agile maneuvers simulating nanosatellite attitude reorientations have been successfully carried out during a European Space Agency (ESA) parabolic flight campaign. The results show that the steering law performs as expected.

Keywords: Control moment gyros, Attitude control, Microgravity, Singularity

Introduction

Control Moment Gyros (CMGs) are actuators that control the attitude of satellites. This technology is particularly fitted to control massive space vehicles like the International Space Station or agile satellites for instance dedicated to Earth observation like Pléiades. Indeed, CMGs commonly present high torque capabilities relatively to their power consumption compared to reaction wheels. However, for nanosatellites, these advantages are not proven especially because very few systems exist on the market [1]. In addition, CMGs present the drawbacks of being complex mechanically and to steer. It can prevent their use in low-cost nanosatellites aimed at being developed rapidly. In this paper, a configuration that has the advantages of redundancy and steering simplicity is presented.
A Control Moment Gyro is composed of a flywheel that spins at a constant rate, creating an angular momentum along an axis $\boldsymbol{x_i}$. Rotating the axis of rotation of the flywheel along an axis $\boldsymbol{z_i}$, named gimbal axis, creates a gyroscopic torque on the $\boldsymbol{y_i}$-axis, as described in Fig. 1.

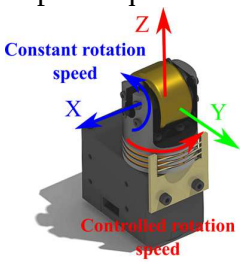

Fig.1: CMG principle

Therefore, instantaneously, a single-gimbal CMG can create a torque along its $\boldsymbol{y_i}$-axis. The torque $\boldsymbol{t_i}$ created is expressed as Eqn 1:

$$\boldsymbol{t_i} = h_f \dot{\sigma}_i \boldsymbol{y_i} \quad (1)$$

With h_f the flywheel angular momentum and $\dot{\sigma}_i$ the gimbal velocity. To control the three axes of a satellite, a cluster of CMGs is needed. Assuming all the CMGs have the same flywheel angular momentum, the total angular momentum $\boldsymbol{h}$ created by the cluster is given in Eqn 2.

$$\boldsymbol{h}(\boldsymbol{\sigma}) = \sum_{i=1}^{n_{CMGs}} h_f \boldsymbol{x_i} = h_f \boldsymbol{X}(\boldsymbol{\sigma}) \begin{bmatrix} 1 \\ \vdots \\ 1 \end{bmatrix} \quad (2)$$

With $\boldsymbol{X}$ the 3-by-n_{CMGs} matrix that concatenates the $\boldsymbol{x_i}$ axes of the CMGs, defined thanks to the gimbal angles σ_i gathered in the n_{CMGs}-by-1 vector $\boldsymbol{\sigma}$. Differentiating Eqn 2 gives the torque created by the cluster in Eqn 3:

$$\boldsymbol{t} = h_f \boldsymbol{Y}(\boldsymbol{\sigma}) \dot{\boldsymbol{\sigma}} \quad (3)$$

With $\boldsymbol{Y}$ the 3-by-n_{CMGs} Jacobian matrix of $\boldsymbol{X}$**.** Designing a steering law for a cluster of CMGs comes down to inverting Eqn 3 in order to find the gimbal velocities $\dot{\boldsymbol{\sigma}}$ to create the required torque $\boldsymbol{t}$ while verifying other constraints. When $\boldsymbol{Y}(\boldsymbol{\sigma})$ is not invertible, then the cluster cannot create a torque along a direction and $\boldsymbol{\sigma}$ is said to be a singular position. Because of this physical characteristics, at least four CMGs are needed in the cluster to add a degree of freedom in steering the CMGs to bypass singularities.

Steering (or allocating) a cluster of CMGs is therefore complex and has been studied for years. H. Kurokawa [2] gives a comprehensive overview of the various types of steering laws designed, and some of them that can be implemented in real-time are recalled here. The first developed consists in doing a pseudo-inversion of Moore-Penrose of Eqn 3. Nevertheless, the command is not robust to singularities, creating large command values to the actuators in these cases. To avoid it, the Singular Robust Inverse method has been developed. It consists in adding a matrix $\boldsymbol{R}$ in the pseudo-inversion to make it always feasible. $\boldsymbol{R}$ can vary with the smallest singular value of $\boldsymbol{Y}$ [3]. Including perturbation terms in $\boldsymbol{R}$ (Perturbed Singular Robust Inverse) prevents the required torque from being in the same direction as the singular ones, enabling the system to go out of singular configurations at no speed [4]. Other allocators include gradient methods to steer the CMGs in the kernel of $\boldsymbol{Y}$ while minimizing a criteria [5]. A method developed in [6] restricts the angular momentum workspace to areas without singularities.

The first part of the paper is dedicated to the choice of the CMG cluster configuration, then to the solution of the allocation problem with this configuration. The second part deals with the experimental setup to explain the hardware and the software developed to carry out the validation of the control loop. Finally, experimental results are shown with two variants of the steering law and from an initial singular position.

Proposed Attitude Control System

Problem statement

The goal is to develop an attitude control system (actuator and control loop) for agile nanosatellites. The choice to study the CMG technology comes from their intrinsic high torque capabilities. The main goals of the study are to find a system which has redundancies to ensure functionality in case of mechanical failures and is simple to steer. Also it is aimed to use the maximal angular momentum capability of the actuators. As for the steering law in particular, calculations in real-time and the possibility to add constraints (saturation, singularity avoidance…) are required. These criteria enforced to design the attitude control are particularly

true for nanosatellites but not limited to. In the two next subsections, the choices are explained regarding these criteria.

CMG cluster configuration chosen

Two main cluster configurations exist: pyramidal or multiple. The last one consists in having the gimbal axes of the CMGs aligned in the same planes. The steering law is simplified but the angular momentum capabilities are lower along some axes, and losing one CMG impacts the remaining capabilities more than in the pyramidal case [2]. In a pyramidal configuration, the CMGs are located on each face of a pyramidal polyhedron, each gimbal axis having a unique orientation. Thus this configuration is chosen. The graph in Fig. 2 shows in blue the values of the maximal angular momentum of an isotropic pyramidal cluster of CMGs with $h_f = 1$ Nms (normalized). The red curve gives the position of the first singularity that cannot be passed through null-motion (elliptic singularity), requiring a dedicated steering law.

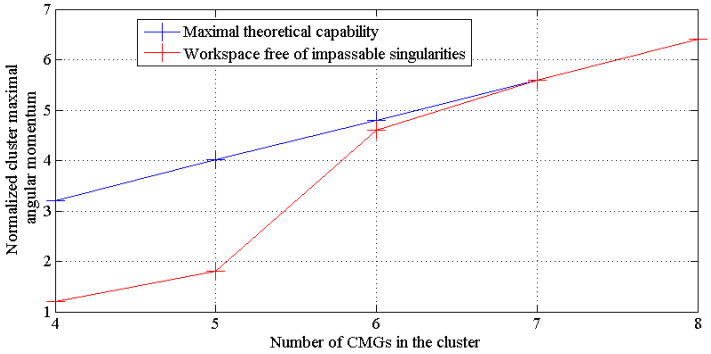

Fig. 2: Workspace free of elliptic singularity compared to the maximal capabilities

This shows that six CMGs is the minimum to have nearly all the angular momentum reachable with a simple steering law. Therefore, this configuration is chosen, even if the compactness of the system is worse than with the usual four-CMG configuration.

Steering law for CMGs

The steering law chosen comes from [7]. It is based on the Extended Kalman Filter (EKF) algorithm which can integrate equality constraints and hierarchize them by scaling their associated covariance. The structure of the algorithm can be kept in case of CMG failures. In addition, it can be calculated in real-time in the satellite, which makes it a suitable structure for our steering law. As seen in the previous subsection, with six CMGs, to reach all the angular momentum only singularities that can be passed through null-motion can be considered. However, in case of CMG failure, the other cases of singularities have to be addressed, like in [8] for instance. As implemented in a calculator, the discrete-time algorithm is given here, with a sample time ΔT. Eqn 3 can be written as Eqn 4 in discrete-time with a limited development of order 2:

$$\Delta \boldsymbol{h} = h_f \boldsymbol{Y}(\boldsymbol{\sigma})\Delta\boldsymbol{\sigma} - \frac{1}{2} h_f \boldsymbol{X}(\boldsymbol{\sigma})(\Delta\boldsymbol{\sigma})^2 = h_f \boldsymbol{M}(\boldsymbol{\sigma}) \begin{bmatrix} \Delta\boldsymbol{\sigma} \\ (\Delta\boldsymbol{\sigma})^2 \end{bmatrix} \tag{4}$$

With $\Delta\boldsymbol{h} = \boldsymbol{h}(t+\Delta T) - \boldsymbol{h}(t)$, $\Delta\boldsymbol{\sigma} = \boldsymbol{\sigma}(t+\Delta T) - \boldsymbol{\sigma}(t)$. The main advantage of this equation is that the matrix $\boldsymbol{M}$ is full-rank whatever $\boldsymbol{\sigma}$, thus it provides a null-motion term. The variables of the EKF and the prediction model are given in Eqn 5.

$$\boldsymbol{v} = \begin{cases} \boldsymbol{v_1} = T_c \Delta\boldsymbol{\sigma}/\Delta T \\ \boldsymbol{v_2} = T_c^2 (\Delta\boldsymbol{\sigma})^2/\Delta T^2 \end{cases} \text{ and } \quad \hat{\boldsymbol{v}}(t+\Delta T) = \begin{cases} \hat{\boldsymbol{v}}_{\boldsymbol{1}}(t+\Delta T) = \hat{\boldsymbol{v}}_{\boldsymbol{1}}(t) \\ \hat{\boldsymbol{v}}_{\boldsymbol{2}}(t+\Delta T) = \hat{\boldsymbol{v}}_{\boldsymbol{2}}(t) \end{cases} \tag{5}$$

With T_c a characteristic time to normalize the variables. The evolution errors are sized in the covariance matrix **Q**. The prediction equations enable to limit the gimbal acceleration. Finally, the measurement equations are given in Eqn 6 with the covariance matrix $\boldsymbol{R}$ associated:

$$\boldsymbol{m} = \begin{cases} \boldsymbol{m_1} = \boldsymbol{t}\frac{T_c}{h_f} = \boldsymbol{Y}(\boldsymbol{\sigma})\boldsymbol{v_1}(t) - \frac{1}{2}\boldsymbol{X}(\boldsymbol{\sigma})\boldsymbol{v_2}(t)\frac{\Delta T}{T_c} + \boldsymbol{\epsilon_{m1}} \\ \boldsymbol{m_2} = \boldsymbol{0} = -\boldsymbol{v_1}(t)^2 + \boldsymbol{v_2}(t) + \boldsymbol{\epsilon_{m2}} \\ \boldsymbol{m_3} = \boldsymbol{0} = \boldsymbol{v_1}(t) + \boldsymbol{\epsilon_{m3}} \end{cases} \quad (6)$$

The convergence of the filter is verified through tuning the maximal and minimal values of the covariance matrices **Q** and **R** thanks to the paper [7]. We then have $\underline{r}\boldsymbol{I} \leq \boldsymbol{R} \leq \bar{r}\boldsymbol{I}$. In this paper we present two cases tested, one with a fixed covariance $\boldsymbol{R_3}$ (associated with the third equation of Eqn 6), and one with a varying covariance value as described in Eqn 7 ($\boldsymbol{R_3}$ is diagonal):

$$\boldsymbol{R_3} = \bar{r}\boldsymbol{I} \text{ or } \boldsymbol{R_3}(i,i) = 10^{\overline{lr} - \dot{\sigma}_i(\overline{lr} - \underline{lr})/\dot{\sigma}_{max}} \quad (7)$$

With $\overline{lr} = \log_{10}\bar{r}$, $\underline{lr} = \log_{10}\underline{r}$ and $\dot{\sigma}_{max}$ the gimbal velocity saturation. This equation enables to vary the covariance to limit the value of $\dot{\sigma}_i$. The lower the covariance value, the higher the importance of the equation, hence in the second case, when the gimbal velocity approaches the saturation limit, this constraint becomes dominant among the other equations. The two steering strategies are tested and compared.

Experimental Setup

Hardware Setup and operations

The developed experiment is described in [9]. It consists in a pyramidal cluster of six in-house CMGs with their power and control electronics. The angle of the pyramid has been chosen to have isotropic angular velocity capabilities. The setup is autonomous in energy and calculates in real-time the control loop thanks to the on-board computer. The sensors are three-axis gyrometers and accelerometers (to record the microgravity level) and a camera not used in the results presented here. The experimentations have been carried out at Novespace, in an ESA parabolic flight campaign thanks to ESA Education Office through the Fly Your Thesis! 2017 programme. During each parabola (microgravity period), the demonstrator is released and then behaves autonomously in free-floating until reaching an obstacle. A parabola lasts around 20 seconds, but the scientific duration was of 11 seconds maximum. 93 parabolas were carried out.

Software control loop

The maneuvers presented in the next section consist in an angular velocity profile calculated on-board. For each parabola, a cluster angular momentum value to be reached is stored. The cluster is initially in gimbal positions such that the sum of the CMG angular momenta is null. When released, the cluster begins by cancelling out the residual demonstrator angular velocity due to the release and the airplane speed. Then, a velocity profile is calculated in real-time to reach the required angular momentum value in a given time. The control law is a proportional gain on the angular velocity measurement, to which a feed-forward action is added to cancel the gyroscopic effects. Then, the torque required is sent to the steering law described in the previous section. The advantage of working with the velocity is to be able to put the cluster near previously calculated singular positions in the gimbal angle domain. Indeed, various initial positions have been tested: the usual one (all the gimbal at 0 rad), one initially far from singularities, and even one beginning in a singular position to check how the cluster escapes. Also, tests with one and two CMGs off have been carried out.

Experimental Results

Three parabola results are given below. Fig. 3 shows a maneuver from a favourable initial position (far from singularity), with a fixed covariance matrix. As shown before, the singularity encountered is near the maximal angular momentum of the cluster, but it still creates a gimbal velocity saturation. To prevent it, the varying covariance has been implemented and the results are shown in Fig. 4.

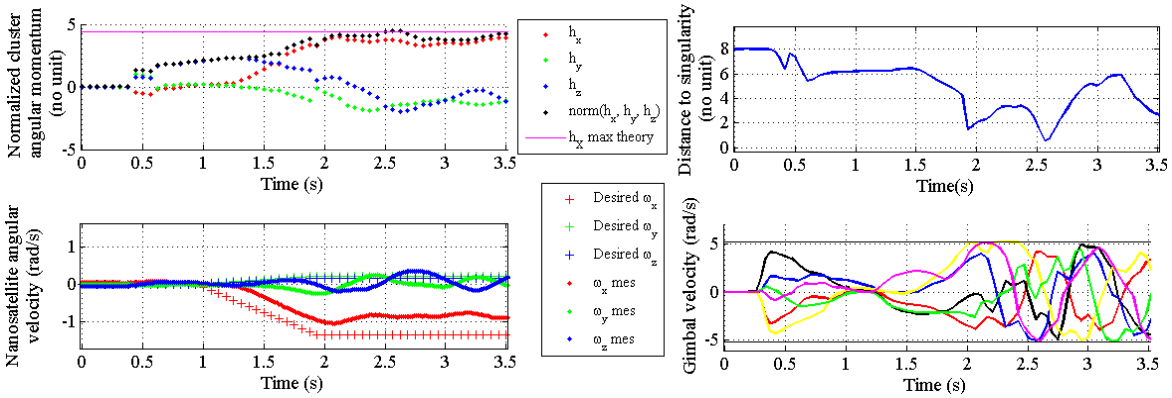

Fig. 3: Experimental results of an X-axis maneuver, with a fixed covariance, from a favourable initial position

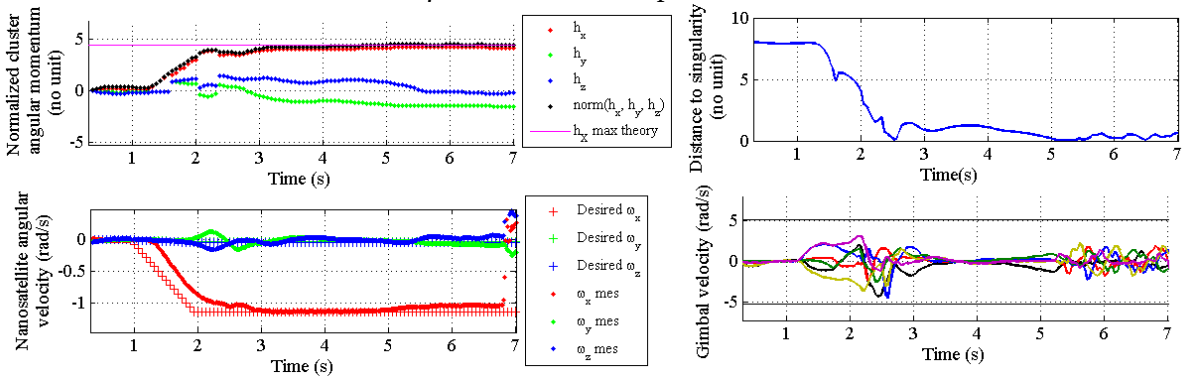

Fig. 4: Experimental results of an X-axis maneuver, with the varying covariance, from a favourable initial position

The gimbal velocities do not saturate during the singularity, but a torque error is created. The gimbal velocities decrease to zero when the set point is reached, showing the stability of the command. Fig. 5 shows the results from a singular initial position.

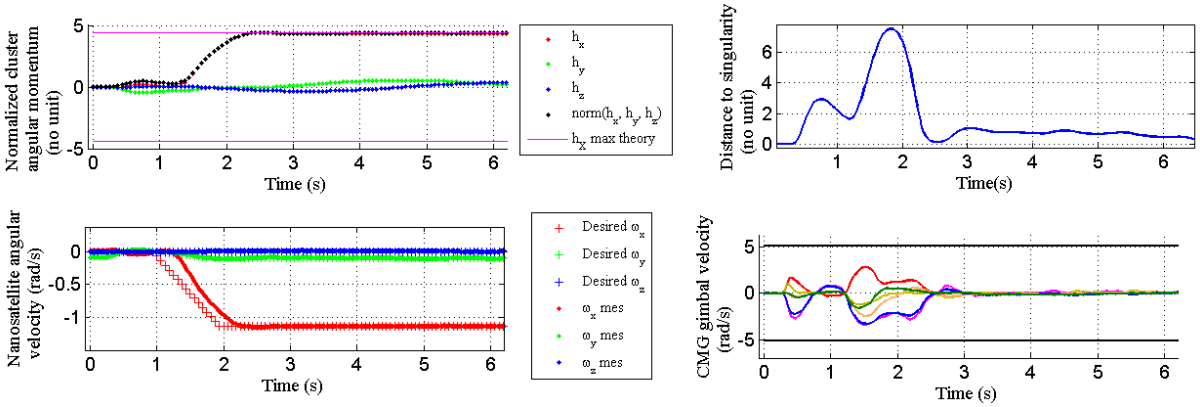

Fig. 5: Experimental results of an X-axis maneuver, with the varying covariance, from a singular initial position

The maximal angular momentum is reached without gimbal saturation even at the beginning, and with stabilisation at the required velocity. Therefore, the “favourable” initial positions are really favourable in the vicinity of the initial gimbal position.

Conclusion

This work presented an attitude control system that verifies our constraints. The experimental results showed in particular the feasibility of implementing the proposed steering law in real-time in a small satellite. Particularly interesting behaviour came out when beginning in initial singular position or when encountering a singularity with the saturation constraint active. Further work will concentrate on demonstrating a typical elliptic singularity avoidance when two CMGs are off, and comparisons with numerical simulations as well as with other steering laws existing in the literature.

Acknowledgements

This work was supported by CNES, ISAE SUPAERO, ONERA and ESA Education Office through the Fly Your Thesis! 2017 programme.

References

1. Votel, R. and Sinclair, D., "Comparison of Control Moment Gyros and Reaction Wheels for Small Earth-Observing Satellites", *26th Annual AIAA/USU Conference on Small Satellites*, 2012.

2. Kurokawa, H., "Survey of Theory and Steering Laws of Single-Gimbal Control Moment Gyros", *Journal of Guidance, Control and Dynamics*, Vol. 30, No. 5, 2007, pp. 1331-1340.

3. Ford, K.A. and Hall, C.D., "Singular Direction Avoidance Steering for Control Moment Gyros", *Journal of Guidance, Control and Dynamics*, Vol. 3, No. 4, 2000, pp. 648-656.

4. Wie, B., Bailey, D. and Heiberg, C.J., "Singularity Robust Steering Logic for Redundant Single-Gimbal Control Moment Gyros", *Journal of Guidance, Control and Dynamics*, Vol. 24, No. 5, 2001, pp. 865-872.

5. Cornick, D.E., "Singularity Avoidance Control Laws for Single-Gimbal Control Moment Gyros", *AIAA Guidance and Control Conference*, 1979, pp. 20-33.

6. Kurokawa, H., "Exact Singularity Avoidance Control of the Pyramid Type CMG System", *AIAA Guidance and Control Conference*, 1994, pp. 170-180.

7. Evain, H., Rognant, M., Alazard, D. and Mignot, J., "Nonlinear Dynamic Inversion for Redundant Systems Using the EKF Formalism", *Proceedings of the 2016 American Control Conference*, 2016, pp 348–353.

8. Evain, H., Rognant, M., Alazard, D. and Mignot, J., "Design of a new real-time steering law for control moment gyro clusters", *10th International ESA Conference on Guidance, Navigation and Control Systems*, Salzbourg, 2017.

9. Evain, H., Solatges, T., Brunet, A., Dias Ribeiro, A., Sipile, L., Rognant, M., Alazard, D. and Mignot, J., "Design and Control of a Nano-Control Moment Gyro Cluster for Experiments in a Parabolic Flight Campaign", *IFAC World Congress GDR MACS session*, 2017.